Chapter 4
Antibody Recognition of Immunodominant Vaccinia Virus Envelope Proteins

Dirk M. Zajonc

Abstract Vaccinia Virus (VACV) is an enveloped double stranded DNA virus and the active ingredient of the smallpox vaccine. The systematic administration of this vaccine led to the eradication of circulating smallpox (variola virus, VARV) from the human population. As a tribute to its success, global immunization was ended in the late 1970s. The efficacy of the vaccine is attributed to a robust production of protective antibodies against several envelope proteins of VACV, which cross-protect against infection with pathogenic VARV. Since global vaccination was ended, most children and young adults do not possess immunity against smallpox. This is a concern, since smallpox is considered a potential bioweapon. Although the smallpox vaccine is considered the gold standard of all vaccines and the targeted antigens have been widely studied, the epitopes that are targeted by the protective antibodies and their mechanism of binding had been, until recently, poorly characterized. Understanding the precise interaction between the antibodies and their epitopes will be helpful in the design of better vaccines against other diseases. In this review we will discuss the structural basis of recognition of the immunodominant VACV antigens A27, A33, D8, and L1 by protective antibodies and discuss potential implications regarding their protective capacity.

Keywords Antibodies • Vaccination • Vaccinia virus • X-ray crystallography • Antibody-antigen complexes

D.M. Zajonc (✉)
Division of Cell Biology, La Jolla Institute for Allergy and Immunology (LJI), La Jolla, CA 92037, USA

Department of Internal Medicine, Faculty of Medicine and Health Sciences, Ghent University, Ghent 9000, Belgium
e-mail: dzajonc@liai.org

J.R. Harris, J. Marles-Wright (eds.), *Macromolecular Protein Complexes*, Subcellular Biochemistry 83, DOI 10.1007/978-3-319-46503-6_4

Abbreviations

VACV	Vaccinia virus
VARV	variola virus
MPXV	monkeypox virus
ECTV	ectromelia virus
MAb	monoclonal antibody
IMV	intracellular mature virus
EEV	extracellular enveloped virus
GAG	glycosaminoglycan
HS	heparan sulfate
CS	chondroitin sulfate
GlcA	glucuronic acid
GalNAc	N-acetyl galactosamine
HC	heavy chain
LC	light chain
CDR	complementarity determining region
H	hydrogen (bond)
vdW	van der Waals
BSA	buried surface area
sc	shape correlation
Fab	fragment of antigen binding
K_D	equilibrium binding constant
EFC	entry fusion complex
SAM	single alanine scanning mutagenesis

4.1 Vaccinia Virus

VACV is a 190 kbp double-stranded DNA virus that encodes more than 200 ORFs. Together with cowpox (CPXV), monkeypox (MPXV), smallpox (VARV) and ectromelia (ECTV), among others, VACV belongs to the genus of orthopox viruses. VACV exists as two different infectious particles, the intracellular mature virus (IMV) and the extracellular enveloped virus (EEV). The IMV expresses and utilizes the adhesion molecules A27, D8, and H3, to bind to cell surface molecular like glycosaminoglycans (GAGs), heparan sulfate (A27 and H3), chondroitin sulfate (D8) (Lin et al. 2000; Hsiao et al. 1998, 1999; Matho et al. 2014). The IMV also expresses A26, which binds to laminin (Chiu et al. 2007). The entry fusion complex of the IMV allows VACV to fuse with the host membrane and ultimately to infect the host cell. Twelve proteins that are conserved across the poxvirus family are required for this process (Ojeda et al. 2006b; Townsley et al. 2005b; Senkevich et al. 2004; Brown et al. 2006; Izmailyan et al. 2006; Ojeda et al. 2006a; Senkevich and Moss 2005; Nichols et al. 2008; Senkevich et al. 2005; Bisht et al. 2008b;

Satheshkumar and Moss 2009; Townsley et al. 2005a). Following viral replication within the host cell, newly synthesized VACV particles exit the cell as EEV particles. In addition to IMV, these particles also have a second host cell-derived lipid bilayer that contains specific EEV envelope proteins, including A33. A33 is an adhesion molecule that binds a receptor of unknown identity and is required for long-range dissemination within the host (Roper et al. 1998; Wolffe et al. 1998, 2001).

Inoculation with VACV elicits neutralizing antibodies against major envelope proteins, including A27, A33, B5, D8, H3, and L1, conferring protection against smallpox (Davies et al. 2005; Davies et al. 2007; Lawrence et al. 2007; Benhnia et al. 2008; Putz et al. 2006). Maximal protection is obtained with vaccines combining membrane proteins from both IMV and EEV. Although the vaccine efficacy has never been precisely measured in controlled experiments, neutralizing antibodies are found up to 30 years after standard immunization. Smallpox was the first disease that had been eradicated through global vaccination efforts, resulting in a termination of the wide-spread vaccination of the general human population (Henderson 2011). Yet, the precise interaction between the antibodies and their epitopes remained poorly understood, until recently.

In this review will focus on the interaction between several murine antibodies and the VACV antigens: A27, A33, D8 and L1, the only antigens for which structural data of the antibody-antigen complex has been obtained to date (Fig. 4.1).

4.2 IMV Antigen A27

A27 is one of the three GAG adhesion molecules (A27, D8, and H3) and binds to heparan sulfate. A27 is a homo-trimeric protein that is attached to the viral membrane by binding to the transmembrane protein A17 through its C-terminal leucine zipper domain (residues 80–101). The GAG binding site is located at the N-terminus of the mature protein (residues 21–30) (Wang et al. 2014; Howard et al. 2008). The central region of A27 consists of a coiled coil domain (residues 43–84), which is used to interact with the membrane fusion suppressor protein, A26, through intermolecular disulfide bond formation (Cys71, Cys72). The crystal structure of an N-terminal fragment of A27, containing the heparan sulfate binding site and coiled coil domain (residues 21–84), has recently been determined, however only the central fragment (residues 47–84) is ordered, suggesting flexibility of the N-terminal GAG binding domain (Chang et al. 2013). The A27 structure illustrates the complexity and antiparallel nature of the A27 homo-trimer, yet structural information about the N-terminal and C-terminal extremities is missing.

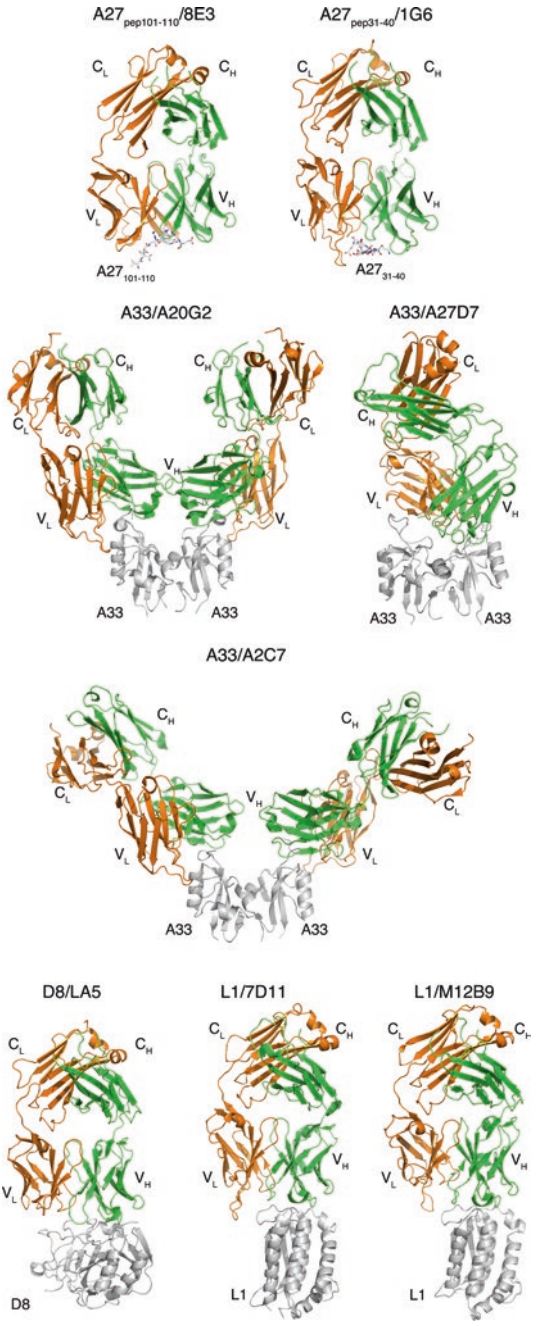

Fig. 4.1 Overview of VACV antigen-antibody (Fab) complexes. The antigens are colored in *grey*, the Fab light (L) chain in *orange* and the Fab heavy (H) chain in *green*. Variable (V) and constant (C) antibody domains are indicated

4.2.1 Anti A27 MAbs

To understand the function of anti-A27 antibodies, especially their protective capacity and their interaction with A27, several murine monoclonal antibodies (MAbs) have been generated and further separated into four distinct specificity groups (Kaever et al. 2016). Three groups (I, III and IV) bind to linear peptides, while group II only binds to VACV lysate and recombinant A27, suggesting it recognized a conformational and discontinuous epitope. Only group I antibodies neutralized MV in a complement-dependent manner and protected against VACV challenge, while a group II mAb protected partially, but did not neutralize (Kaever et al. 2016). The epitope for group I mAbs was mapped to a region adjacent to the GAG binding site and suggested that group I mAbs could potentially interfere with cellular adhesion of A27, while the group IV antibodies bound to the remote C-terminal extremity of A27 and were not neutralizing (Kaever et al. 2016). For details on antibody composition and structure see (Sundberg and Mariuzza 2002; Kumagai and Tsumoto 2001).

4.2.2 Crystal Structure of the $A27_{peptide31–40}$ -1G6 Complex

The crystal structure of the neutralizing group I MAb, 1G6, bound to the A27 peptide "KREAIVKADE" illustrating that both light and heavy chains of the antibody are equally important in binding the peptide (Table 4.1 and Fig. 4.2). The peptide is bound in a crevice formed between the complementarity determining region (CDR) L1 loop and the H2 loop and was supported mainly by the underlying H3 loop. The H chain buried 385 $Å^2$ on the peptide, while the L chain buried 366 $Å^2$. 1G6 formed polar contacts (hydrogen bonds and salt bridges) with seven amino acids of the A27 peptide, with five residues of the L chain interacting with four amino acids of the antigen (Arg32, Glu33, Ala34, and Asp39), while five residues of the H chain interacted with four amino acids (Lys37, Ala38, Asp39, Glu40) of the antigen (Table 4.1, Fig. 4.2). L1 appears to form the majority of polar interactions with A27, while the H chain uses H2 and H3 to bind the antigen. H1 is the only CDR that does not contact the peptide.

The structural data corroborated the alanine scanning mutagenesis, which identified several important side chain interactions of the peptide antigen with the antibody. A27 residues Glu33, Ile35, Val36, Lys37, and Asp39 were sensitive to alanine substitution. Peptide residues Glu33 and Asp39 formed a hydrogen (H) bond with L1 residues Ser32 and Tyr37, respectively, while Asp39 also forms a salt bridge with H2 residue Lys55. Peptide residues Lys37 formed a salt bridge with both H2 residues Asp59 and Asp61, while Glu40 forms salt bridge with H3 residue Arg104 and an H bond with Tyr106. Disruption of any of these contacts led to loss of binding, suggesting that these interactions were equally important for binding (Kaever et al. 2016). I35 and V36 are hydrophobic amino acids and their side chains do not

Table 4.1 Structural analysis of antibody-peptide binding

Antibody	**8E3**	**1G6**	**A20G2**	**A27D7**	**A2C7**	**LA5**	**7D11**	**M12B9**
Antigen	A27 peptide 101–110	A27 peptide 31–40	A33 monomer	A33 dimer	A33 monomer	D8	L1	L1
V-Gene and allele, J-Gene and allele	IGHV2–4-1*01, IGHJ3*01	IGHV8–8*01, IGHJ4*01	IGHV5–12*02, IGHJ4*01	IGHV2–6-5*01, IGHJ2*01	IGHV5–12*02, IGHJ4*01	IGHV1S127*01, IGHJ1*01	IGHV1S26*01, IGHJ3*01	IGHV1S26*01, IGHJ3*01
	IGLV3*01, IGLJ2*01	IGKV1–110*01, IGKJ1*01	IGKV1–133*01, IGKJ2*01	IGKV4–91*01, IGKJ4*01	IGKV1–110*01, IGKJ1*01	IGKV4–55*01, IGKJ5*01	IGKV8–21*01, IGKJ1*01	IGKV1–110*01, IGKJ1*01
Isotype	IgG2a	IgG2a	IgG2a	IgG2a	IgG2b	IgG2a	IgG2a	IgG2a
Total BSA Å^2 (antibody/antigen)	HC: 355	HC: 385	HC: 430	HC: 630	HC: 334	HC: 1872	HC: 1340	HC: 1366
	LC: 480	LC: 366	LC: 435	LC: 525	LC: 365	LC: 562	LC: 225	LC: 219
Shape complementarity (0–1)	n.d.	n.d.	HC: 0.68	HC: 0.71	HC: 0.67	HC: 0.62	HC: 0.65	HC: 0.70
			LC: 0.69	LC: 0.74	LC: 0.68	LC: n.d.	LC: 0.26	LC: 0.62
Contact CDRs[a]	**L1, L2, L3, H1, H2**, H3	**L1, L2**, L3, **H2, H3**	**L1, L3, H1, H2**, H3	**L1**, **L2, L3, H1, H2, H3**	**L1**, L2, **L3, H1, H2, H3**	L1, **L3, H1, H2, H3**	L1, **H1, H2, H3**	L1, L3, **H1, H2, H3**
Number of Antigen contact residues	6	7	16	24	11	23	12	16
Contact overview[b]	HC: 6 HB, (vdW n.d.)	HC: 3 HB, 5 SB, (vdW n.d.)	HC: 8 HB, 2 SB, 66 vdW	HC: 14 HB, 1 SB, 80 vdW	HC: 4 HB, 47 vdW	HC: 16 HB/ 11 SB/ 115 vdW	HC: 8 HB/ 2 SB/ (vdW n.c.)	HC: 11 HB/ 5 SB/ 99 vdW
	LC: 5 HB, 4 SB, (vdW n.d)	LC: 7 HB, 4 SB, (vdW n.d.)	LC: 8 HB, 52 vdW	LC: 10 HB, 66 vdW	LC: 7 HB, 1 SB, 53 vdW	LC: 1 HB/ 15vdW	LC: (vdW n.c.)	LC: 1 HB/ 1 SB

Neutralizing in vitro	No	Yes	Yes	Yes	Yes	Yes	Yes	Yes
Protect against[c] VACV / ECTV	No/n.t.	Yes/n.t.	Yes/ No	Yes/Yes	Yes/No	n.t./n.t.	Yes/n.t.	Yes/No
KD (SPR/BLI)	n.t.	n.t.	66 pM (BLI)	14 nM (BLI)	65 pM (BLI)	0.18 nM (SPR)	n.t.	91 nM (BLI)

[a]CDRs/ residues in bold form multiple contacts
[b]*HB* Hydrogen bond, *SB* salt bridge, *vdW* van der Waals, *n.d.* not determined, *n.c.* not counted
[c]*n.t.*= not tested

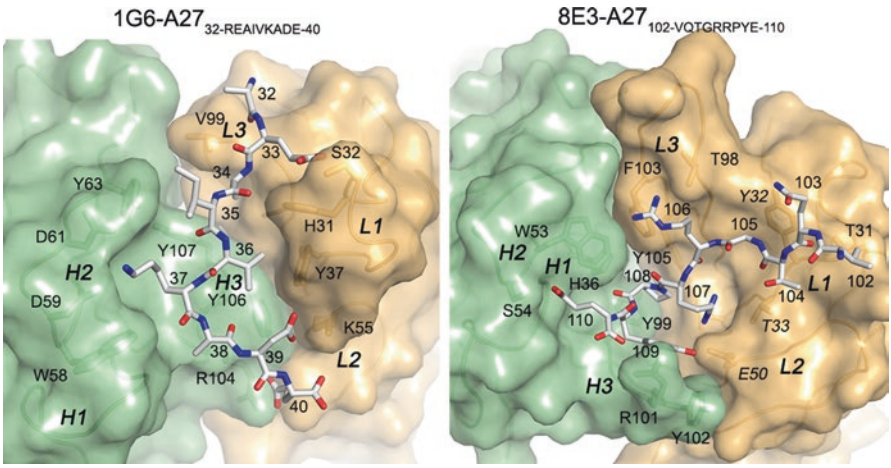

Fig. 4.2 Antibody binding to A27 peptides. The molecular surfaces of the antigen binding sites illustrate intimate binding to A27 peptides. Several contact residues of the Fab are labeled in italics, while peptide residues are numbered according to amino acid position in the A27 protein. Heavy chain in *green* and light chain in *orange*. Peptide as *grey sticks*. CDR loops in *italics*

engage in polar interactions, however Ile33 packed against H2 residue Tyr63, while Val36 packs against L1 residues His31 and Tyr37. These hydrophobic interactions appear to be critical to the overall stability of the complex (Fig. 4.2).

4.2.3 Crystal Structure of the A27$_{peptide101–110}$ -8E3 Complex

The group IV MAb 8E3 bound to the A27 peptide DVQTGRRPYE surprisingly with a higher contribution of the L chain than the H chain. However, in contrast to the MAb 1G6, 8E3 forms the binding side perpendicular to the H/L chain interface, while 1G6 bound the peptide in a crevice formed between the H and L chain. As a result, 8E3 binds the N-terminal residues exclusively with the L chain and the C-terminal residues exclusively with the H chain, while for 1G6 certain residues can interact with both antibody chains simultaneously (Fig. 4.2). The H chain of 8E3 interacted less broadly with the antigen and buried 355 Å^2, while the L chain buried 480 Å^2 on the peptide (Table 4.1).

The antibody 8E3 formed polar contacts with seven amino acids of the antigen. Six residues of the L chain interacted with five amino acids of the peptide (Gln103, Thr104, Arg106, Arg107, and Tyr109), while four residues of the H chain interacted with two amino acids (Pro108 and Glu110) of the peptide (Table 4.1, Fig. 4.2). While the L chain appeared to make more contacts with the peptide overall, alanine scanning of the peptide suggested that the N-terminal half of the peptide was not forming specific interactions with the antibody. H bond interactions with A27 residues Gln103 and Gly105 are formed with backbone oxygen groups, indicating that

they are independent of the amino acid sequence. Gly105 to alanine substitution likely induced a steric clash with the antibody surface. As a result the amino acids that were forming specific interactions with the antibody were located within the C-terminal half and include Arg107, Tyr109 and possibly Glu110. Pro108 to alanine exchange likely also induces a steric clash with 8E3. Arg107 and Tyr109 are involved in both a salt bridge and H bond with L2 residue Glu50, which therefore seems to be a major hot spot for binding the antigen, while Glu110 of the peptide formed a H bond with H2 residues Ser54 and H3 residue Arg101, which appeared to be less crucial for binding based on the alanine scanning data (Kaever et al. 2016).

A27 is one of the immunodominant antigens of VACV and antibodies targeting A27 have been extensively studied (Meyer et al. 1994; Rodriguez and Esteban 1987; Rodriguez et al. 1985). Especially group I antibodies had been previously identified and the epitope mapped to the heparan binding domain (Meyer et al. 1994). Therefore, the group I epitope appears to constitute a major binding site for eliciting protective antibodies such as 1G6.

4.3 EEV Antigen A33

A33 is expressed on the EEV membrane as a 23 kDa, homodimeric type II transmembrane protein that undergoes both O- and N-glycosylation (Isaacs et al. 1992; Roper et al. 1996; Payne 1992). A33 controls the incorporation of A36 into the EEV particle and subsequently the production of actin tails. Therefore, A33 plays an important role in effective cell-to-cell spread within the host (Roper et al. 1998; Wolffe et al. 1998, 2001). A33 is also required for proper trafficking of the VACV antigen B5 to the EEV-specific membrane and proper formation of infectious EEV (Wolffe et al. 2001; Chan and Ward 2010). A33 contains a membrane-proximal cysteine on the A33 ectodomain that forms an intermolecular disulfide bridge. However, this cysteine is not required for the production of infectious extracellular virus (Chan et al. 2010). The crystal structure of the ectodomain of A33 revealed an unusual C-type lectin-fold domain, similar in overall architecture to several NK cell ligands (Su et al. 2010).

4.3.1 Anti A33 MAbs

Recent characterization of a panel of anti A33 antibodies using a peptide ELISA indicated that all the anti-A33 MAbs obtained by immunizing mice with live VACV bound only to recombinant A33 but not to any linear peptide, in contrast to most antibodies targeting A27 (Matho et al. 2015). Interestingly, the three antibodies: A2C7, A27D7, and A20G2, which had been characterized in more detail, bound to A33 with different stoichiometries. A single A27D7 Fab bound to one A33 dimer, while A2C7 and A20G2 each bound with one Fab to one A33 subunit (2 Fab's per

A33 dimer) (Matho et al. 2015). While all three MAbs were neutralizing *in vitro*, protected against intranasal VACV challenge *in vivo*, A27D7 also protected mice against ectromelia challenge, identifying A27D7 as a potent cross-species orthopox virus neutralizing antibody (Matho et al. 2015).

4.3.2 Crystal Structure of the A33-A2C7 Complex

The A33/A2C7 complex shows two Fab molecules symmetrically bound to the A33 dimer (Fig. 4.1). Each A2C7- Fab molecule elicits, therefore, identical contacts with a discontinuous and conformational epitope at the membrane-distal extremity of each A33 subunit (Fig. 4.3). The A33 monomer is bound in a deep cavity formed by both L and H chain, with L1 and H2 forming the rim of a binding cup. The L chain buried 365 Å^2 on A33, while the H chain buried a total of 334 Å^2 between A33, leading to a total BSA of 699 Å^2 between Fab and A33, which corresponds to only around 5% of total protein surfaces. The size of the binding interface is comparable to the peptide binding anti A27 MAbs but considerably smaller than the typical range found in antibody-protein antigen complexes (1400–1700 Å^2 BSA), (Davies et al. 1990). Despite recognizing a rather small epitope, A2C7 used sixteen residues (eight from each L and H chain) to interact with eleven A33 residues. Similar to the peptide-specific anti A27 MAbs, both L and H chain of A2C7 appeared to be equally important in antigen binding.

Shape correlation (Sc) measures the geometric surface complementarity of protein-protein interfaces and reflects their specificity (Lawrence and Colman 1993). Both heavy and light chains appeared to bind with high specificity to the antigen (Sc = 0.67 and 068, respectively). For antigen-antibody interfaces, Sc values of 0.64–0.68 (Jones and Thornton 1996) have been reported, illustrating that the A2C7/A33 interaction is very specific. This interface is held together by an extensive network of hydrogen bonds and salt bridges involving every CDR loop (Matho et al. 2015). Gln173 is a major contact residue of the A2C7 epitope, as it reaches into the base of the A2C7 binding cup and intersects with of almost every CDR loop (Fig. 4.3). It forms multiple hydrogen bonds via its backbone and side chain (H1, H2, H3, and L3). Replacing Gln173 with arginine led to a complete loss of A2C7 binding. Since the Gln173Arg substitution is found in ECTV the binding data suggested that A2C7 would be unable to protect against ectromelia challenge and no protection was indeed found using an ectromelia challenge model (Matho et al. 2015). A33 residue Asp170 is located on a flexible loop and is contacted by both H and L chain. It forms a salt bridge with L2 residue Lys55 and a hydrogen bond with L1 residue Tyr32. However, the Asp170Ala mutation did not affect the binding affinity of A2C7-MAb, suggesting it is not a critical binding residue (Matho et al. 2015).

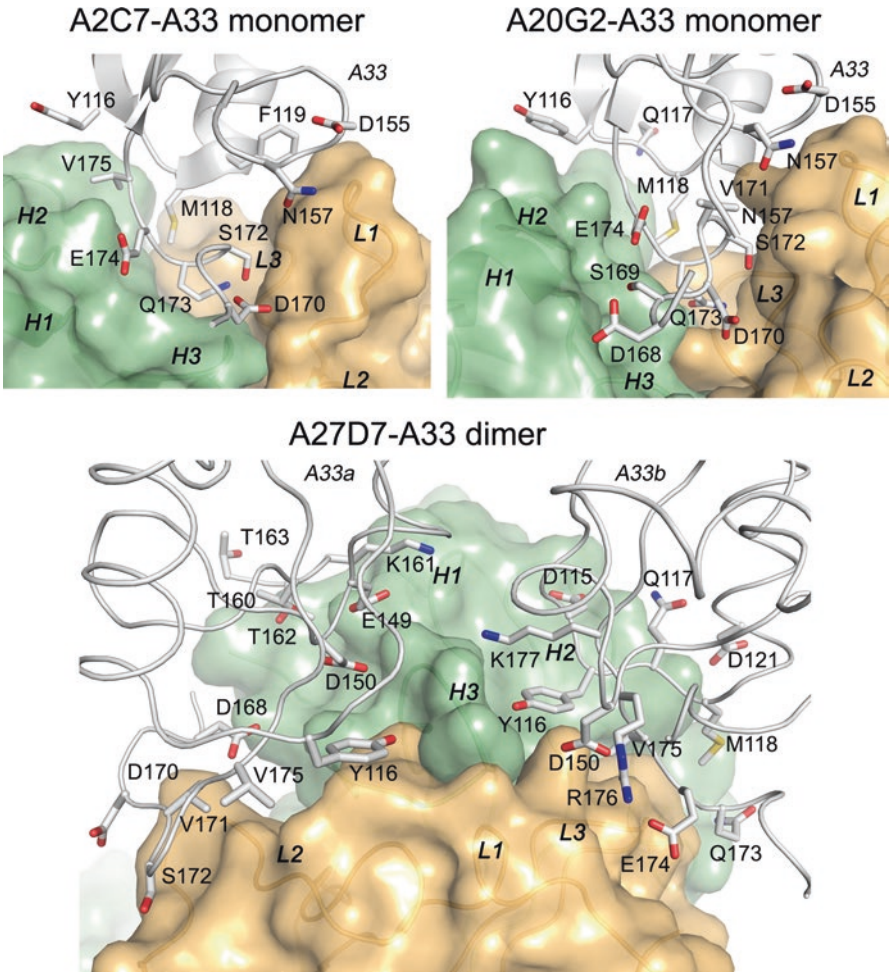

Fig. 4.3 A33-antibody interfaces. Fab A2C7 and A20G2 bind the A33 monomer in a crevice formed between L (*orange*) and H (*green*) chain, while A27D7 binds the A33 dimer. Heavy chain in *green* and light chain in *orange*. A33 in *grey*. CDR loops in *italics*

4.3.3 Crystal Structure of the A33-A20G2 Complex

A20G2 also bound with 1 Fab molecule to one A33 monomer (two Fab's per A33 dimer, Fig. 4.1). A20G2 targets a similar epitope compared to A2C7. Sixteen residues of each A33 subunit were in contact with sixteen residues of the A20G2 Fab (Table 4.1). Compared to the binging cup formed by A2C7, A20G2 is open ended at both ends, explaining the larger binding surface. Both H and L chain grasp the tip of each A33 subunit similar to a tweezer, and each chain buried roughly 430 Å^2 on A33. The Sc value is 0.68 and 0.69 for both antibody/antigen binding interfaces

(Table 4.1). Despite numerous amino acid differences in the CDRs, A20G2 approaches the antigen with an overall similar topology compared to A2C7, with the exception of CDRs L2 and H3. This is reflected in an overall change in binding angle (Fig. 4.1). L1 plays a major role in A33 binding for both A2C7 and A20G2, as it clamps onto one side of each A33 subunit (A33 residues Phe119, Asp155, Gly156, Asn157, Asp170, and Ser172, while Ser154 and Asn157 were exclusive to A20G2) (Fig. 4.3). L3 sits at the base of the binding site, and H1 and H2 target a similar epitope at the top edges of A33. In both complexes, Gln173 is inserted deep into the center of the binding site. Similar to A2C7, the Gln173Arg mutation also fully abrogated A20G2 binding, explaining the inability of this MAb to protect against ectromelia challenge (Matho et al. 2015). In addition, the Asp170Ala mutation did not have any impact on binding of A20G2 to A33, similar to A2C7. The A33 mutation Leu118Arg that is located on both epitopes fully impaired A2C7 binding, while not affecting binding of A20G2. This was likely due to a clash with L3 of A2C7, which approached A33 from a different angle. In conclusion, A2C7 and A20G2 target similar but not identical epitopes mostly due to sequence differences within H3 and L3 (Matho et al. 2015).

4.3.4 Crystal Structure of the A33-A27D7 Complex

A27D7 is unique in its binding to A33. A single A27D7-Fab bound at the A33 dimer interface, with the L and H chains contacted both A33 subunits (Figs. 4.1 and 4.3). The binding interfaces for both L and H chains were considerably larger compared to A2C7 and A20G2 (LC = 525.3 Å^2, HC = 630.2 Å^2) for a total of 1155.5 Å^2 (A27D7-A33 dimer). Sc values of 0.71 and 0.74 were very high and indicate a highly specific binding interaction (Table 4.1) (Matho et al. 2015).

Eighteen residues of the H chain contacted sixteen A33 residues, while fifteen residues of the L chain contacted twelve A33 residues (Matho et al. 2015). CDR H1 interacted only with one A33 subunit, while CDR H2 interacted only with the other A33 subunit of the dimer. Among the many hydrogen bonds and salt bridges formed between A27D7 and A33, a few residues that appeared to make important contacts were targeted for alanine scanning mutagenesis. Lys161 formed a salt bridge with H1 residue Asp31. Asp115 is a central residue of the H2 interface, as it formed six potential hydrogen bonds with H2 residues Gly53, Gly54, Gly55, and Thr56. Surprisingly, the Lys161Ala mutation did not impair A27D7 binding, while the Asp115Ala mutation only slightly affected A33 binding. CDR H3 is centrally positioned in the A33 dimer groove, and contacted residues of both A33 subunits. H3 formed three distinct hydrogen bonds between Ala97, Ser98 and Lys177 of A33. The third hydrogen bond is formed between A33 residue Tyr116 and H3 residue Tyr99 (Matho et al. 2015).

The A27D7 light chain does not elicit any salt bridge with A33, and its interaction with the antigen is mostly driven by van der Waals contacts. In particular L2 and L3 each interact specifically with only one of the A33 subunits (Fig. 4.3). L1 is

relatively short compared to group II MAbs A20G2 and A2C7 (12 vs. 16 residues). A single L1 residue, Tyr32, formed one hydrogen bond with Asp150 and also accounted for all vdW contacts with a single A33 subunit. L2 interacts solely with the other A33 subunit, forming a total of two hydrogen bonds and 30 vdW contacts. CDR L3 (Ser92 and Leu94) formed an extensive hydrogen bond network with A33 residues Gln173, Glu174, Val175 and Arg176. However, A27D7 bound the A33 mutant Gln173Arg still with high affinity, suggesting that the many contacts formed between A27D7 and A33 could compensate for the various single amino acid substitutions on A33, in contrast to the antibodies A2C7 and A20G2, which both failed to bind the Gln173Ala mutant (Matho et al. 2015). Since A27D7 binding appeared resistant to single alanine-scanning mutagenesis, A33 residues that were bound by the antibody on both A33 subunits were targeted by mutagenesis, since these mutations would disrupt interactions on both A33 monomers. Tyr116, Asp150, and Val175 form contacts with the Fab in both A33 subunits, and among those, Tyr116 was chosen for mutagenesis. The Tyr116Ala mutation led to a significant decrease in binding affinity, however, still retained sub nanomolar affinity (Matho et al. 2015). Even double mutants that had significantly reduced binding affinity compared to wildtype still bound with low nanomolar affinity, suggesting that a large number of energetically favorable interactions still remained intact and enabled the specific binding interaction. Based on the binding data, A33 mutants were created that mimicked the epitope of the orthopox strains such as cowpox Brighton (CPXV-Br), MPXV, and ECTV. The A33 variant Gln117Lys/Leu118Ser both mimicked the epitope of CPXV and MPXV, while the A33 variant Gln117Lys/Leu118Ser/Gln173Arg was specific for ECTV. Both antibodies A2C7 and A20G2 failed to bind to the ECTV variant, while A20G2 still bound with a ~9-fold lower affinity to the CPXV/MPXV variant. As expected however, A27D7 was able to bind both A33 variants with high affinity and as predicted from the binding data was able to protect mice against ectromelia challenge, suggesting that this antibody is a potent cross-species orthopox virus neutralizing antibody (Matho et al. 2015).

4.4 IMV Antigen D8

D8 is a 32 kDa type 1 membrane protein of the IMV that binds to cell surface chondroitin sulfate (CS) but not to HS (Hsiao et al. 1999). The large N-terminal domain of D8 shares significant homology to human carbonic anhydrases and adopts a typical CAH fold. This N-terminal domain is characterized by a centrally located positively charged crevice that is lined by several lysine, histidine and arginine residues, suitable for the binding of CS. Using a combination of site directed mutagenesis and antibody cross-blocking, the positively charged crevice was identified as the GAG binding site (Matho et al. 2014; Matho et al. 2012). The last thirty residues of the ectodomain were disordered in the crystal structure and contain an extracellular membrane-proximal cysteine that is used for disulfide-linked dimerization. Recombinant full-length D8 forms a hexamer in solution, in which 3

disulfide-linked dimers non-covalently associate, while the N-terminal GAG binding domain only forms monomers (Matho et al. 2014, 2012). Using a glycan microarray, CS-E [(GlcA-4S,6S-GalNAc)n] was identified as the preferred molecular species of chondroitin sulfate that is bound by D8 (Matho et al. 2014). While the biological significance of hexamerization is not clear, it was suggested that it would increase binding affinity to CS for viral adhesion the host cell (Matho et al. 2014).

4.4.1 Anti D8 Antibodies

Recently a panel of murine monoclonal anti D8 antibodies were characterized and further separated into four different specificity groups, based on their cross-blocking ability (Sela-Culang et al. 2014). The grouping suggested that D8 provided a large surface area that was targeted differently by these antibodies. Peptide ELISA further suggested that group II antibodies targeted a linear epitope called peptide 58 (residues 91–110), while groups I, III and IV targeted a conformational epitope (Sela-Culang et al. 2014). Using EM, the binding sites for group I, II, and III were identified, while a crystal structure was obtained for the group IV antibody LA5 bound to D8. Since only the group IV antibody fully blocked binding of D8 to CS-E (Matho et al. 2014), this antibody will be discussed in more detail.

4.4.2 Crystal Structure of the D8-LA5 Complex

LA5 is an IgG2a isotype (Meng et al. 2011), and its Fab bound recombinant D8 with high affinity (KD = 0.18 nM, Table 4.1). The binding interface between D8 and LA5 was very large, with a total buried surface area of 2434 Å^2. The H chain dominated the binding footprint, with a total of 1872 Å^2 buried surface, which is in contrast to the 562 Å^2 covered by the L chain (Table 4.1). Since the shape complementarity was not very high, water molecules were found especially between D8 and the L chain of LA5 to increase the binding specificity (Matho et al. 2012). The LA5 D8 epitope was formed by twenty-three residues covering the entire sequence of D8 (Gln3, Leu5, Thr39, Gly40, Lys41, Arg44, Lys108, Asn145, Ile174, Asn175, His176, Ser177, Ser204, Leu205, Ile215, Glu217, Tyr219, Arg220, Asn221, Tyr223, Lys224, plus N218 and N226 if including water-mediated contacts), with seven residues sharing contacts with at least two CDR's of LA5 (Thr39, Lys41, Asn145, Asn175, His176, Glu217 and Arg220). Interestingly, the D8 epitope residues Arg44, Lys48 and Arg220 were also involved in CS-E binding, since replacement with alanine either reduced (Arg220Ala) or fully abrogated (Arg44Ala/Arg220Ala and Lys48Ala/Arg220Ala) D8 binding to CS-E. Together with the CS-E microarray data, this demonstrated that LA5 binding overlapped with the binding site for CS-E and that several D8 contact for both CS-E and LA5 were shared. Eighteen residues of LA5

contacted the antigen D8, from five of the six CDRs of LA5. While the L chain only formed one polar interaction (H-bond) and 15 vdW contacts, the H chain bound through an intricate network of polar interactions (16 hydrogen bonds and 11 salt bridges), with an additional 115 vdW interactions contributing to the vast majority of the Fab-Ag interactions (Table 4.1). CDR H2 and H3 seemed to contribute equally in terms of the number of interactions with D8, while H1 contributes the least to the binding interface, with only three H-bonds and 43 vdW interactions.

4.4.3 Possible Function of LA5

Most noticeable, LA5 bound with CDR H1, H2, and H3 directly above the GAG binding crevice of D8. Previous CS-E docking experiments placed the carboxylate of glucuronic acid (GlcA) pointing down into the binding crevice, while the 4′ and 6′ sulfates of the N-acetyl galactosamine (GalNAc) were mostly placed at the top of the binding crevice, where its negative charge would be neutralized by the various electrostatic interactions with the positively-charged groove lining residues of D8 (Fig. 4.4). The residues that when replaced with alanine impacted D8 binding to CS-E (Lys41, Arg44 and Arg220), all formed salt-bridges in the D8-CS-E model, corroborating their importance in CS-E binding (Matho et al. 2014). Based on the combined structural and biochemical data Lys48 and Lys98 likely form the entrance portal to the crevice, while Arg220 and Lys41 form the exit portal. In the computational model, CS-E binding extended beyond these portals and the CS-E ends sat flat above the surface of D8, forming less specific polar contacts. However, the exact length of the CS-E molecule that interacts with D8 had not been experimentally determined (Fig. 4.4). Computational docking further suggested the exit portal to form multiple contacts with the sulfates of CS-E, especially both 4′ and 6′ sulfates bound to Arg220, while at the exit portal, only a single salt-bridge was formed with GlcA, while the 6′ sulfate sat deep inside the crevice. Obviously structural data is necessary to really determine the precise interactions between D8 and CS-E. However, the current model suggested that the exit portal of the D8 crevice is structurally optimized for the binding of CS-E, while the exit portal is structurally slightly more promiscuous in its binding specificity (Fig. 4.4). Strikingly in the LA5-D8 structure, a triad of negatively charged residues of CDR H2 (Asp53, Glu56 and Glu58) bound inside the positively charge crevice of D8 (Fig. 4.4), likely mimicking the negatively charged 4′-, and 6′ sulfate groups. Strategies of true receptor-mimicry have been found especially in antibodies targeting the sialic acid binding site of influenza hemagglutinin, where an aspartate residue of the antibody is in an identical position compared to the carboxylate of sialic acid (Lee et al. 2014).

In conclusion, the binding site of LA5 on D8 overlapped directly with the predicted binding site of CS-E and would likely outcompete CS-E binding to D8 through its high, sub-nanomolar binding affinity or block initial binding to CS-E. As a result, LA5 likely prevents D8 binding to CS on host cells, thus leading to a

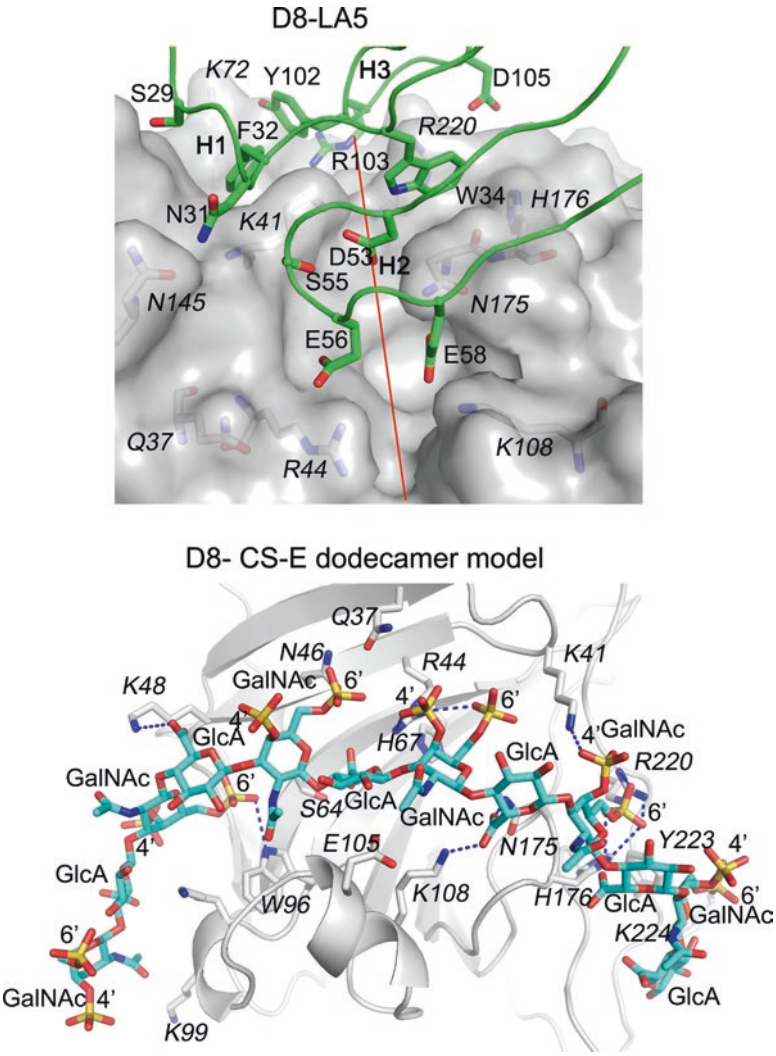

Fig. 4.4 LA5 binding to D8 and D8/CS-E model. The Fab of LA5 binds with the three CDRs of the H chain (H1, H2, and H3 in *green*) directly above the CS-E binding crevice (*red line*) of D8 (*grey surface*). Computational model of a CS-E dodecamer (*cyan sticks*) binding to D8 (*grey cartoon*). D8 residues in *italics*, LA5 residues in regular font

reduced infectivity through the D8/CS axis. This is exemplified by a reduced VACV virulence in BALB/c mice using D8 deletion strains (Rodriguez et al. 1992). However, loss of D8 activity, can be compensated for by VACV binding to HS through the adhesion molecules A27 and H3, since D8-negative virus replicates efficiently in cultured cells (Niles and Seto 1988).

4.5 IMV Antigen L1

L1 is a 250-amino-acid myristoylated protein with a C-terminal transmembrane domain that spans residues 186–204 (Franke et al. 1990; Su et al. 2005). L1 forms a bundle of α-helices that pack against a pair of two-stranded β-sheets (Su et al. 2005). L1 associates with the virus-encoded multiprotein entry-fusion complex (EFC) and plays an essential role in viral entry (Bisht et al. 2008a). It is an immunodominant neutralizing antibody target in mice, though it is a less common target in humans (Benhnia et al. 2008). A VACV L1 mutant had been described that escaped neutralization by the antibody 2D5 and where residue Asp35 had been replaced with asparagine (Ichihashi and Oie 1996). Interestingly, the residue Asp35 in question, is located at the tip of L1, where various loops connect the β-strands and α-helices, and a common target of neutralizing antibody responses (Kaever et al. 2014; Su et al. 2005, 2007). However, not all MAbs that target Asp35 can bind the Asp35Asn escape mutant (Kaever et al. 2014; Su et al. 2007).

4.5.1 Anti L1 Antibodies

Murine anti L1 MAbs had been previously characterized by several labs and identified at least three different specificity groups (Aldaz-Carroll et al. 2005; Ichihashi and Oie 1996; Kaever et al. 2014; Su et al. 2007; Wolffe et al. 1995). In one study, the three antibody groups had been characterized side by side (Kaever et al. 2014). While the majority of antibodies obtained in this study belonged to group I, which targeted a conformational and discontinuous epitope containing the above mentioned Asp35, group II and III MAbs recognized a unique epitope. The group II MAb 8C8 bound a conformational epitope that is separate from the group I MAbs but otherwise unknown, while the group III MAb 39D4 targeted a linear epitope (residues 121–140) that overlapped with a previously identified epitope of L1 (residues 118–128) (Aldaz-Carroll et al. 2005). The group I MAbs neutralized IMV *in vitro* and *in vivo* in the absence of complement. The group II MAb 8C8 failed to neutralize MV, likely because its epitope was not well exposed on the virion (Kaever et al. 2014). The group III MAb 39D4 only neutralized less than 20% and neutralization efficacy could not be increased by the addition of complement, which this antibody can fix. In addition, both group II and III MAbs bound recombinant L1 with greatly reduced binding affinity compared to a the group I MAb M12B9 (K_D = 17 and 32 nM vs. 0.091) (Kaever et al. 2014). The two group I antibodies 7D11 and M12B9 that were produced by different labs had both been characterized structurally and, surprisingly, recognize a highly conserved epitope centered around Asp35 of L1 and have very similar H chain sequences (Kaever et al. 2014; Su et al. 2007).

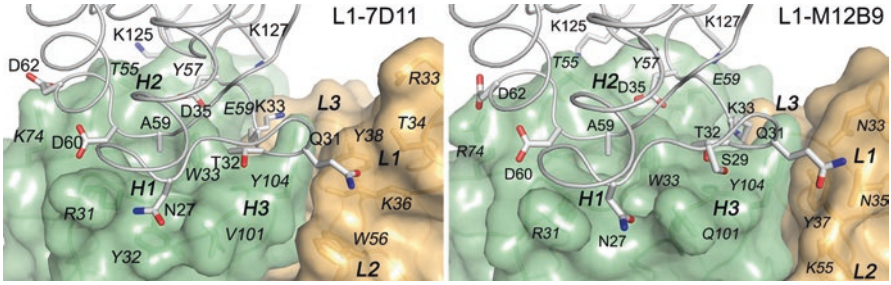

Fig. 4.5 M12B9 and 7D11 binding to the L1 antigen. Antibodies 7D11 and M12B9 bind to VACV-L1 with highly similar binding chemistries, predominantly using the H chain (*green*). Light chain in *orange*, VACV-L1 in *grey*. CDR loops and Fab residues in *italics*. VACV-L1 residues in regular font

4.5.2 Crystal Structure of the L1-7D11 Complex

L1 was the first VACV antigen for which a crystal structure in complex with a Fab was obtained (Su et al. 2007). The antibody 7D11 is a group I antibody and the crystal structure revealed a very H chain centric footprint on top of the L1 molecule (Fig. 4.1). 7D11 binds to four long loops that connect the bundle of helices at the tip of L1, presumably away from the viral membrane. The H chain buried a total of 1340 Å^2, while the L chain participated little in overall binding and buried 225 Å^2 on L1. Shape complementarity is 0.65 for the H chain and 0.26 for the L chain, correlating with an H chain centric footprint. L1 residues Asn27, Gln31, Thr32, Lys33, Asp35, Ser58, Ala59, Asp60, Ala61, Asp62, and Lys125 are bound by the M12B9 heavy chain using vdW interactions, while L1 residues Lys33, Asp35, Ala59, Asp60 also form eight hydrogen bonds and two salt bridges with CDR1–3 residues of the H chain (Table 4.1, Fig. 4.5). Interestingly 7D11 binds to the VCV escape mutant Asp35Asn (Su et al. 2007), which is also found in ECTV. However, whether 7D11 protects against ectromelia challenge is currently unknown.

4.5.3 Crystal Structure of the L1-M12B9 Complex

M12B9 also belongs to the group I antibodies and not surprisingly has a highly similar H chain sequence compare to 7D11, while the L chain is very different (Table 4.1). VACV-L1 residues Glu25, Asn27, Ala28, Ser29, Gln31, Thr32, Lys33, Asp35, Ser58, Ala59, Asp60, Ala61, Asp62, Lys125, Lys127, and Ser153 are bound directly by the M12B9 heavy chain (Fig. 4.5) (Kaever et al. 2014). The heavy chain forms a total of eleven H-bonds, five salt bridges, and ninety-nine van der Waals (vdW) interactions. The H chain buried 1366 Å^2 surface between VACV-L1 and has a shape complementarity of 0.70, while the LC buried a total 219 Å^2 with a shape complementarity of 0.62. In total, the M12B9 light chain formed one potential salt

bridge and one hydrogen bond involving L chain residue Asp98 (CDR L3), Asn34 (CDR L1) and VACV-L1 residue Lys33 and Gln31, respectively, while in the 7D11/L1 structure, there were no interactions between the light chain and VACV-L1 within 4 Å distance (Su et al. 2007). Surprisingly, however, the escape mutant Asp35Asn was resistant to neutralization by any group I MAbs characterized in this particular study, suggesting an inability of these MAbs to bind to Asn35 instead of Asp35 (Kaever et al. 2014). While binding of M12B9 to the recombinant VACV-L1 containing the Aps35Asn was not tested, no binding of M12B9 to the VACV-L1 mutant Asp35Ala was observed, demonstrating the importance of Asp35 for group I MAb binding. Since ECTV contains the Asp35Asn variation, and M12B9 did not protect against ECTV challenge it could be speculated that M12B9 does not bind the Asp35Asn variant found in the ECTV L1 ortholog (EVM072). However, that would contrast 7D11 binding, which was not affected by the same mutation.

4.5.4 7D11 Versus M12B9 Comparison

Both L1-7D11 and L1-M12B9 complex structures bound a highly conserved epitope on L1, correlating well with the high sequence similarity of the H chains (Kaever et al. 2014). The overall H chain sequence identity was 83% and differences are found in the framework residues and CDR H3, while H1 and H2 are very conserved (only 1 amino acid difference). As a result, the structures superimposed well with a low root mean square deviation of 1.00 Å. The only gross structural differences are within the H3 loop (only 30% conserved sequence) (Kaever et al. 2014). While M12B9 formed a hydrogen bond between CDR H3 residue Gln101 and Asn27, 7D11 formed a salt-bridge between CDR H3 residue Asp102 and L1 residue Lys33. Since the Ans27Ala mutant retained full binding to M12B9, this contact did not appear important for M12B9 binding, while on the other hand the additional salt bridge (adjacent to Asp35 of L1), formed by 7D11 could compensate for Asp35Asn mutation to retain binding (Fig. 4.5). Both MAbs, however, share the majority of polar interactions that are formed by CDRs H1 and H2, while CDR H3 adopted a similar orientation in both complexes but almost exclusively contacted L1 through non-directed vdW interactions (Kaever et al. 2014).

4.6 Concluding Remarks

Antibody responses against VACV had been structurally characterized for the antigens A27, A33, D8 and L1. Antibodies were either obtained by immunizing mice with VACV with or without following boost with recombinant protein or by immunizing mice only with recombinant protein. Immunizing mice with VACV resembles closely the natural antibody response following infection. During that response the obtained antibodies exhibit certain features that appear to be driven by the nature

of the antigen. The majority of studied antibodies appeared to target a conformational and discontinuous, rather than a liner peptide, with the exception of A27. For A27 only few antibodies had been obtained that require folded A27 protein for binding. A27 is a rather small protein and contains α-helical segments and disordered domains (Chang et al. 2013). Except for the antiparallel trimerization that creates a composite binding surface for antibodies, the A27 structure itself is linear and it might very well be that several of the linear peptides recapitulate the tertiary structure found in the A27 protein. Both L and H chain contributed equally to the binding, a feature that has been described for antibodies binding small molecule, peptides and haptens (Kumagai and Tsumoto 2001).

For A33, two groups of antibodies have been characterized. Those that bind with one Fab to one A33 monomer, essentially having identical epitopes on each A33 monomer, and those antibodies that recognize a composite and unique binding surface in the A33 dimer, to which only a single Fab can bind. The latter binding mode is characterized by a larger binding foot print (buried surface area), which also appears to be more resistant to single alanine scanning mutagenesis (SAM). SAM has been a technique to identify epitope residues but depending on the antibody, will only identify hot spot residues and not residues that are not crucial for antibody binding. Since the A33 dimer presented a rather small surface area and unique protein shape, most antibodies that target A33 cross-blocked each other and, hence, antibody cross-blocking is not a powerful tool for epitope identification for small protein antigens. For A33, both L and H chain contribute equally to the binding and employ a "tweezer-like" binding mode, essentially grabbing onto A33 from both sides. This was largely due to longer CDR loops (specially CDR L1) that formed a central cavity in the antibody paratope (the antibody surface that binds the epitope of the antigen).

D8 is unique in that it presented a large surface for antibodies to bind. Not surprisingly the most antibody specificity groups are found for anti D8 MAbs. While some MAbs target the CS-E receptor binding site on D8, more or less mimicking the negatively charged ligand with an array of aspartate and glutamate residues, other MAbs bind to different D8 surfaces. The study of anti D8 antibodies revealed that there is no preferred or immunogenic site on D8. Antibodies are found targeting any accessible site on D8 and all anti D8 antibodies bound the N-terminal GAG binding domain. No antibody has been identified to date that binds to the C-terminal stalk region that is necessary for oligomerization. This suggests that the C-terminal domain is not accessible in VACV and a weak target for antibody responses. Interestingly, antibodies that target D8 rely excessively on the H chain in recognizing the antigen, with little contribution from the L chain. This is surprising given the fact, that the antibody LA5 has the largest binding footprint of all anti VACV antibodies for which structural information has been acquired. Similarly, anti-L1 MAbs bind their antigen predominantly with the H chain, at the tip of the molecule, where L1 itself forms 4 different loops that are contacted by the antibodies. Since L1 is part of the EFC, neutralizing anti-L1 MAbs do not require the presence of complement for efficient neutralization, while MAbs recognizing A27, A33, and D8 all

require the presence of complement for neutralization, which increases both viral coating with complement and is required for opsonization.

Acknowledgements I would like to thank Bjoern Peters, Yan Xiang, Shane Crotty and Mark Buller for a terrific collaboration and all lab members, especially Michael H. Matho, Tom Kaever, Xiangzhi Meng and Andrew Schlossman without whom the studies would have been nearly impossible. Many thanks also to Yan Xiang for critically reading the manuscript. This project has been funded in whole or in part with federal funds from the National Institute of Allergy and Infectious Diseases, National Institutes of Health, Department of Health and Human Services, under contract no. HHSN272200900048C

References

Aldaz-Carroll L, Whitbeck JC, Ponce de Leon M, Lou H, Pannell LK, Lebowitz J, Fogg C, White CL, Moss B, Cohen GH, Eisenberg RJ (2005) Physical and immunological characterization of a recombinant secreted form of the membrane protein encoded by the vaccinia virus L1R gene. Virology 341(1):59–71. doi:S0042-6822(05)00416-2 [pii]10.1016/j.virol.2005.07.006

Benhnia MR, McCausland MM, Su HP, Singh K, Hoffmann J, Davies DH, Felgner PL, Head S, Sette A, Garboczi DN, Crotty S (2008) Redundancy and plasticity of neutralizing antibody responses are cornerstone attributes of the human immune response to the smallpox vaccine. J Virol 82(7):3751–3768. doi:10.1128/JVI.02244-07

Bisht H, Weisberg AS, Moss B (2008a) Vaccinia virus l1 protein is required for cell entry and membrane fusion. J Virol 82(17):8687–8694. doi:10.1128/JVI.00852-08

Bisht H, Weisberg AS, Moss B (2008b) Vaccinia virus l1 protein is required for cell entry and membrane fusion. J Virol 82(17):8687–8694. doi:10.1128/JVI.00852-08

Brown E, Senkevich TG, Moss B (2006) Vaccinia virus F9 virion membrane protein is required for entry but not virus assembly, in contrast to the related L1 protein. J Virol 80(19):9455–9464. doi:10.1128/JVI.01149-06

Chan WM, Ward BM (2010) There is an A33-dependent mechanism for the incorporation of B5-GFP into vaccinia virus extracellular enveloped virions. Virology 402(1):83–93. doi:10.1016/j.virol.2010.03.017

Chan WM, Kalkanoglu AE, Ward BM (2010) The inability of vaccinia virus A33R protein to form intermolecular disulfide-bonded homodimers does not affect the production of infectious extracellular virus. Virology 408(1):109–118. doi:10.1016/j.virol.2010.09.021

Chang TH, Chang SJ, Hsieh FL, Ko TP, Lin CT, Ho MR, Wang I, Hsu ST, Guo RT, Chang W, Wang AH (2013) Crystal structure of vaccinia viral A27 protein reveals a novel structure critical for its function and complex formation with A26 protein. PLoS Pathog 9(8):e1003563. doi:10.1371/journal.ppat.1003563

Chiu WL, Lin CL, Yang MH, Tzou DL, Chang W (2007) Vaccinia virus 4c (A26L) protein on intracellular mature virus binds to the extracellular cellular matrix laminin. J Virol 81(5):2149–2157. doi:10.1128/JVI.02302-06

Davies DR, Padlan EA, Sheriff S (1990) Antibody-antigen complexes. Annu Rev Biochem 59:439–473. doi:10.1146/annurev.bi.59.070190.002255

Davies DH, Liang X, Hernandez JE, Randall A, Hirst S, Mu Y, Romero KM, Nguyen TT, Kalantari-Dehaghi M, Crotty S, Baldi P, Villarreal LP, Felgner PL (2005) Profiling the humoral immune response to infection by using proteome microarrays: high-throughput vaccine and diagnostic antigen discovery. Proc Natl Acad Sci U S A 102(3):547–552. doi:10.1073/pnas.0408782102

Davies DH, Molina DM, Wrammert J, Miller J, Hirst S, Mu Y, Pablo J, Unal B, Nakajima-Sasaki R, Liang X, Crotty S, Karem KL, Damon IK, Ahmed R, Villarreal L, Felgner PL (2007) Proteome-wide analysis of the serological response to vaccinia and smallpox. Proteomics 7(10):1678–1686. doi:10.1002/pmic.200600926

Franke CA, Wilson EM, Hruby DE (1990) Use of a cell-free system to identify the vaccinia virus L1R gene product as the major late myristylated virion protein M25. J Virol 64(12):5988–5996

Henderson DA (2011) The eradication of smallpox--an overview of the past, present, and future. Vaccine 29(Suppl 4):D7–D9. doi:10.1016/j.vaccine.2011.06.080

Howard AR, Senkevich TG, Moss B (2008) Vaccinia virus A26 and A27 proteins form a stable complex tethered to mature virions by association with the A17 transmembrane protein. J Virol 82(24):12384–12391. doi:10.1128/JVI.01524-08

Hsiao JC, Chung CS, Chang W (1998) Cell surface proteoglycans are necessary for A27L protein-mediated cell fusion: identification of the N-terminal region of A27L protein as the glycosaminoglycan-binding domain. J Virol 72(10):8374–8379

Hsiao JC, Chung CS, Chang W (1999) Vaccinia virus envelope D8L protein binds to cell surface chondroitin sulfate and mediates the adsorption of intracellular mature virions to cells. J Virol 73(10):8750–8761

Ichihashi Y, Oie M (1996) Neutralizing epitope on penetration protein of vaccinia virus. Virology 220(2):491–494. doi:10.1006/viro.1996.0337

Isaacs SN, Wolffe EJ, Payne LG, Moss B (1992) Characterization of a vaccinia virus-encoded 42-kilodalton class I membrane glycoprotein component of the extracellular virus envelope. J Virol 66(12):7217–7224

Izmailyan RA, Huang CY, Mohammad S, Isaacs SN, Chang W (2006) The envelope G3 L protein is essential for entry of vaccinia virus into host cells. J Virol 80(17):8402–8410. doi:10.1128/JVI.00624-06

Jones S, Thornton JM (1996) Principles of protein-protein interactions. Proc Natl Acad Sci U S A 93(1):13–20

Kaever T, Meng X, Matho MH, Schlossman A, Li S, Sela-Culang I, Ofran Y, Buller M, Crump RW, Parker S, Frazier A, Crotty S, Zajonc DM, Peters B, Xiang Y (2014) Potent neutralization of vaccinia virus by divergent murine antibodies targeting a common site of vulnerability in L1 protein. J Virol 88(19):11339–11355. doi:10.1128/JVI.01491-14

Kaever T, Matho MH, Meng X, Crickard L, Schlossman A, Xiang Y, Crotty S, Peters B, Zajonc DM (2016) Linear epitopes in A27 are targets of protective antibodies induced by vaccination against smallpox. J Virol. doi:10.1128/JVI.02878-15

Kumagai I, Tsumoto K (2001) Antigen–Antibody Binding. In: eLS. John Wiley & Sons, Ltd. doi:10.1002/9780470015902.a0001117.pub2

Lawrence MC, Colman PM (1993) Shape complementarity at protein/protein interfaces. J Mol Biol 234(4):946–950. doi:S0022-2836(83)71648-7[pii]10.1006/jmbi.1993.1648

Lawrence SJ, Lottenbach KR, Newman FK, Buller RM, Bellone CJ, Chen JJ, Cohen GH, Eisenberg RJ, Belshe RB, Stanley SL Jr, Frey SE (2007) Antibody responses to vaccinia membrane proteins after smallpox vaccination. J Inf Dis 196(2):220–229. doi:10.1086/518793

Lee PS, Ohshima N, Stanfield RL, Yu W, Iba Y, Okuno Y, Kurosawa Y, Wilson IA (2014) Receptor mimicry by antibody F045-092 facilitates universal binding to the H3 subtype of influenza virus. Nat Commun 5:3614. doi:10.1038/ncomms4614

Lin CL, Chung CS, Heine HG, Chang W (2000) Vaccinia virus envelope H3L protein binds to cell surface heparan sulfate and is important for intracellular mature virion morphogenesis and virus infection in vitro and in vivo. J Virol 74(7):3353–3365

Matho MH, Maybeno M, Benhnia MR, Becker D, Meng X, Xiang Y, Crotty S, Peters B, Zajonc DM (2012) Structural and biochemical characterization of the vaccinia virus envelope protein D8 and its recognition by the antibody LA5. J Virol 86(15):8050–8058. doi:10.1128/JVI.00836-12

Matho MH, de Val N, Miller GM, Brown J, Schlossman A, Meng X, Crotty S, Peters B, Xiang Y, Hsieh-Wilson LC, Ward AB, Zajonc DM (2014) Murine anti-vaccinia virus D8 antibodies target different epitopes and differ in their ability to block D8 binding to CS-E. PLoS Pathog 10(12):e1004495. doi:10.1371/journal.ppat.1004495

Matho MH, Schlossman A, Meng X, Benhnia MR, Kaever T, Buller M, Doronin K, Parker S, Peters B, Crotty S, Xiang Y, Zajonc DM (2015) Structural and functional characterization of anti-a33 antibodies reveal a potent cross-species orthopoxviruses neutralizer. PLoS Pathog 11(9):e1005148. doi:10.1371/journal.ppat.1005148

Meng X, Zhong Y, Embry A, Yan B, Lu S, Zhong G, Xiang Y (2011) Generation and characterization of a large panel of murine monoclonal antibodies against vaccinia virus. Virology 409(2):271–279. doi:10.1016/j.virol.2010.10.019

Meyer H, Osterrieder N, Czerny CP (1994) Identification of binding sites for neutralizing monoclonal antibodies on the 14-kDa fusion protein of orthopox viruses. Virology 200(2):778–783. doi:10.1006/viro.1994.1241

Nichols RJ, Stanitsa E, Unger B, Traktman P (2008) The vaccinia virus gene I2L encodes a membrane protein with an essential role in virion entry. J Virol 82(20):10247–10261. doi:10.1128/JVI.01035-08

Niles EG, Seto J (1988) Vaccinia virus gene D8 encodes a virion transmembrane protein. J Virol 62(10):3772–3778

Ojeda S, Domi A, Moss B (2006a) Vaccinia virus G9 protein is an essential component of the poxvirus entry-fusion complex. J Virol 80(19):9822–9830. doi:10.1128/JVI.00987-06

Ojeda S, Senkevich TG, Moss B (2006b) Entry of vaccinia virus and cell-cell fusion require a highly conserved cysteine-rich membrane protein encoded by the A16L gene. J Virol 80(1):51–61. doi:10.1128/JVI.80.1.51-61.2006

Payne LG (1992) Characterization of vaccinia virus glycoproteins by monoclonal antibody precipitation. Virology 187(1):251–260

Putz MM, Midgley CM, Law M, Smith GL (2006) Quantification of antibody responses against multiple antigens of the two infectious forms of Vaccinia virus provides a benchmark for smallpox vaccination. Nat Med 12(11):1310–1315. doi:10.1038/nm1457

Rodriguez JF, Esteban M (1987) Mapping and nucleotide sequence of the vaccinia virus gene that encodes a 14-kilodalton fusion protein. J Virol 61(11):3550–3554

Rodriguez JF, Janeczko R, Esteban M (1985) Isolation and characterization of neutralizing monoclonal antibodies to vaccinia virus. J Virol 56(2):482–488

Rodriguez JR, Rodriguez D, Esteban M (1992) Insertional inactivation of the vaccinia virus 32-kilodalton gene is associated with attenuation in mice and reduction of viral gene expression in polarized epithelial cells. J Virol 66(1):183–189

Roper RL, Payne LG, Moss B (1996) Extracellular vaccinia virus envelope glycoprotein encoded by the A33R gene. J Virol 70(6):3753–3762

Roper RL, Wolffe EJ, Weisberg A, Moss B (1998) The envelope protein encoded by the A33R gene is required for formation of actin-containing microvilli and efficient cell-to-cell spread of vaccinia virus. J Virol 72(5):4192–4204

Satheshkumar PS, Moss B (2009) Characterization of a newly identified 35-amino-acid component of the vaccinia virus entry/fusion complex conserved in all chordopoxviruses. J Virol 83(24):12822–12832. doi:10.1128/JVI.01744-09

Sela-Culang I, Benhnia MR, Matho MH, Kaever T, Maybeno M, Schlossman A, Nimrod G, Li S, Xiang Y, Zajonc D, Crotty S, Ofran Y, Peters B (2014) Using a combined computational-experimental approach to predict antibody-specific B cell epitopes. Structure. doi:10.1016/j.str.2014.02.003

Senkevich TG, Moss B (2005) Vaccinia virus H2 protein is an essential component of a complex involved in virus entry and cell-cell fusion. J Virol 79(8):4744–4754. doi:10.1128/JVI.79.8.4744-4754.2005

Senkevich TG, Ward BM, Moss B (2004) Vaccinia virus A28L gene encodes an essential protein component of the virion membrane with intramolecular disulfide bonds formed by the viral cytoplasmic redox pathway. J Virol 78(5):2348–2356

Senkevich TG, Ojeda S, Townsley A, Nelson GE, Moss B (2005) Poxvirus multiprotein entry-fusion complex. Pro Natl Acad Sci U S A 102(51):18572–18577. doi:10.1073/pnas.0509239102

Su HP, Garman SC, Allison TJ, Fogg C, Moss B, Garboczi DN (2005) The 1.51-Angstrom structure of the poxvirus L1 protein, a target of potent neutralizing antibodies. Proc Natl Acad Sci U S A 102(12):4240–4245. doi:10.1073/pnas.0501103102

Su HP, Golden JW, Gittis AG, Hooper JW, Garboczi DN (2007) Structural basis for the binding of the neutralizing antibody, 7D11, to the poxvirus L1 protein. Virology 368 (2):331–341. doi:S0042-6822(07)00439-4[pii]10.1016/j.virol.2007.06.042 [doi]

Su HP, Singh K, Gittis AG, Garboczi DN (2010) The structure of the poxvirus A33 protein reveals a dimer of unique C-type lectin-like domains. J Virol 84, 2009/12/25 edn. doi:10.1128/JVI.02247–09

Sundberg EJ, Mariuzza RA (2002) Molecular recognition in antibody-antigen complexes. Adv Protein Chem 61:119–160

Townsley AC, Senkevich TG, Moss B (2005a) The product of the vaccinia virus L5R gene is a fourth membrane protein encoded by all poxviruses that is required for cell entry and cell-cell fusion. J Virol 79(17):10988–10998. doi:10.1128/JVI.79.17.10988-10998.2005

Townsley AC, Senkevich TG, Moss B (2005b) Vaccinia virus A21 virion membrane protein is required for cell entry and fusion. J Virol 79(15):9458–9469. doi:10.1128/JVI.79.15.9458-9469.2005

Wang DR, Hsiao JC, Wong CH, Li GC, Lin SC, Yu SS, Chen W, Chang W, Tzou DL (2014) Vaccinia viral protein A27 is anchored to the viral membrane via a cooperative interaction with viral membrane protein A17. J Biol Chem 289(10):6639–6655. doi:10.1074/jbc.M114.547372

Wolffe EJ, Vijaya S, Moss B (1995) A myristylated membrane protein encoded by the vaccinia virus L1R open reading frame is the target of potent neutralizing monoclonal antibodies. Virology 211(1):53–63. doi:10.1006/viro.1995.1378

Wolffe EJ, Weisberg AS, Moss B (1998) Role for the vaccinia virus A36R outer envelope protein in the formation of virus-tipped actin-containing microvilli and cell-to-cell virus spread. Virology 244(1):20–26. doi:10.1006/viro.1998.9103

Wolffe EJ, Weisberg AS, Moss B (2001) The vaccinia virus A33R protein provides a chaperone function for viral membrane localization and tyrosine phosphorylation of the A36R protein. J Virol 75(1):303–310. doi:10.1128/JVI.75.1.303-310.2001